

Electronic Supplementary Information

# Tailored Synthesis of Molecularly-Thin Platinum Nanosheets Using Designed 2D Surfactant Solids

Eisuke Yamamoto<sup>a,b,\*</sup>, Akiko Suzuki<sup>a</sup>, Makoto Kobayashi<sup>a</sup> and Minoru Osada<sup>a,c\*</sup>

<sup>a</sup>*Department of Materials Chemistry & Institute of Materials and Systems for Sustainability (IMaSS), Nagoya University, Nagoya 464-8601, Japan.*

<sup>b</sup>*Precursory Research for Embryonic Science and Technology (PRESTO), Japan Science and Technology Agency (JST), Saitama 332-0012, Japan.*

<sup>c</sup>*International Center for Materials Nanoarchitectonics (WPI-MANA), National Institute for Materials Science (NIMS), Tsukuba 305-0044, Japan.*

**Fig.S 1 The optical microscope images of the 2D surfactant crystals prepared at different conditions: (a)The sample prepared by drying the liquid droplet. The samples prepared by spin coating at (b) 1500 rpm, (c) 2000 rpm, (d) 3000 rpm, (e) 4000 rpm, and (f) 5000 rpm..... 3**

**Fig.S 2 (a) and (b) XRD patterns, (c) and (d) Raman spectra, and (e), (f) and (g) XPS spectra of the samples: (a), (c), and (e) 2D surfactant crystals, (b), (d), and (f) 2D Pt complex, and (g) Pt metal nanosheets..... 3**

**Fig.S 3 Appearances of the (a) 2D surfactant crystals and (b) those after calcination at 450 °C for removal of the organic species..... 4**

**Fig.S 4 Appearances of the (a) 2D surfactant crystals and (b) those after reduction process without UV-ozone treatment..... 4**

**Fig.S 5 The AFM images of the Pt metal nanosheets reduced at (a) 200, (b) 300 and (c) 120 °C. (d) XPS spectrum of the Pt metal nanosheets reduced at 120 °C for 5 h..... 4**

**Fig.S 6 (a) AFM images and (b) its high-resolution image of Pt metal nanosheets synthesized on mica substrate. The images were observed by Cypher VRS equipment for clear observation of the**

<b>nanostructure.....</b>	<b>5</b>
<b>Fig.S 7 (a), (c), (e) and (g) AFM images and (b), (d), (f) and (h) height profiles of Pt metal nanosheets synthesized with various conditions: (a) and (b) nanosheet prepared on MgO substrate. (c) and (d) nanosheet prepared on Al<sub>2</sub>O<sub>3</sub> substrate. (e) and (f) nanosheet prepared using cetyltrimethylammonium chloride as a metal complex precursor. ....</b>	<b>6</b>
<b>Fig.S 8 The AFM images of the Pt metal nanosheets used for monitoring the thicknesses.....</b>	<b>6</b>
<b>Fig.S 9 (a)AFM image and (b) height profile of the Pt metal nanosheet with large lateral size.....</b>	<b>7</b>
<b>Fig.S 10 (a) and (b) AFM images, (c)XPS spectrum and (d) in-plane XRD pattern of Pt metal nanosheet after calcination. ....</b>	<b>7</b>
<b>Fig.S 11 (a) SEM image (b) XRD pattern, (c) Raman spectrum, and (d) XANES spectrum of the surfactant crystals prepared using H<sub>2</sub>Pt(IV)Cl<sub>6</sub>. ....</b>	<b>8</b>
<b>Fig.S 12 A moiety of [(C<sub>16</sub>H<sub>33</sub>)N(CH<sub>3</sub>)<sub>3</sub>]<sub>2</sub>[PtX<sub>4</sub>] (X = Br or Cl). Displacement ellipsoids are drawn at the 90% probability level. ....</b>	<b>10</b>

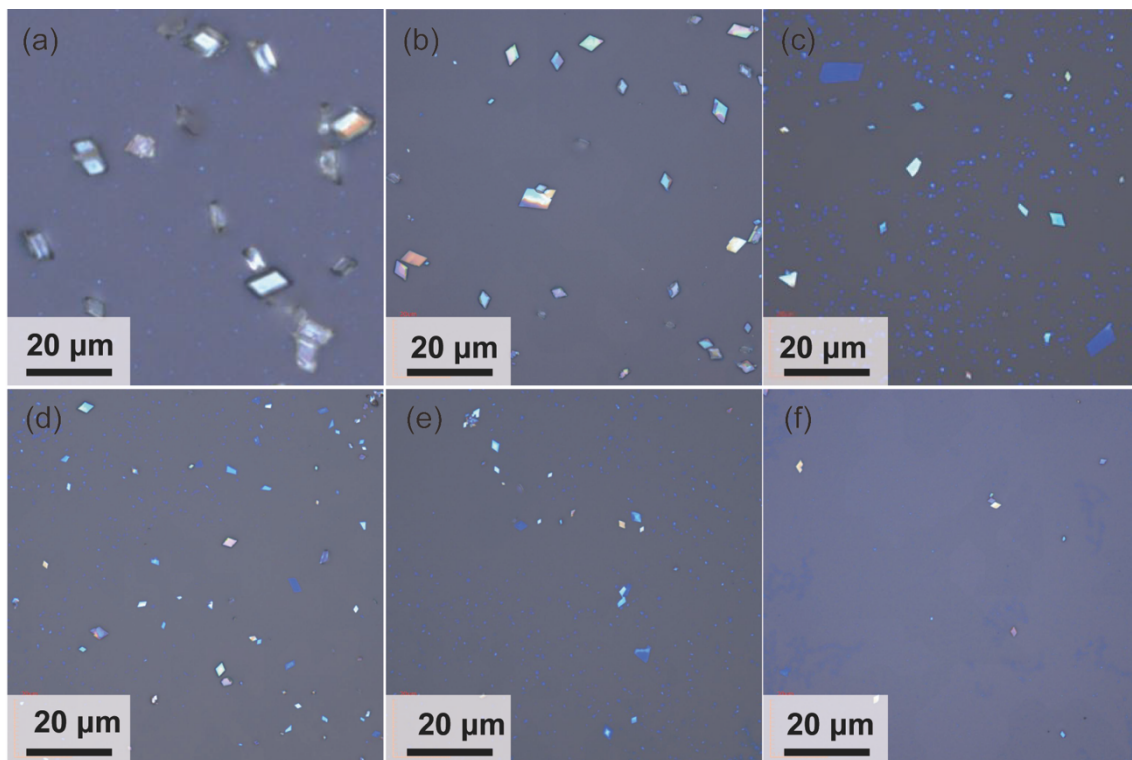


Fig.S 1 The optical microscope images of the 2D surfactant crystals prepared at different conditions: (a)The sample prepared by drying the liquid droplet. The samples prepared by spin coating at (b) 1500 rpm, (c) 2000 rpm, (d) 3000 rpm, (e) 4000 rpm, and (f) 5000 rpm.

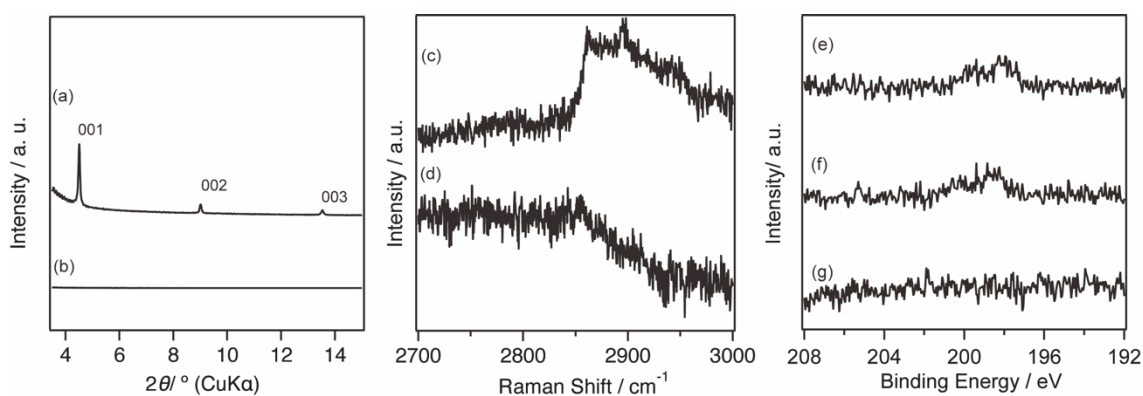


Fig.S 2 (a) and (b) XRD patterns, (c) and (d) Raman spectra, and (e), (f) and (g) XPS spectra of the samples: (a), (c), and (e) 2D surfactant crystals, (b), (d), and (f) 2D Pt complex, and (g) Pt metal nanosheets.

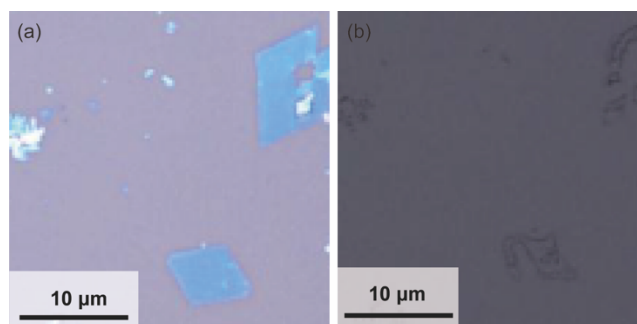


Fig.S 3 Appearances of the (a) 2D surfactant crystals and (b) those after calcination at 450 °C for removal of the organic species.

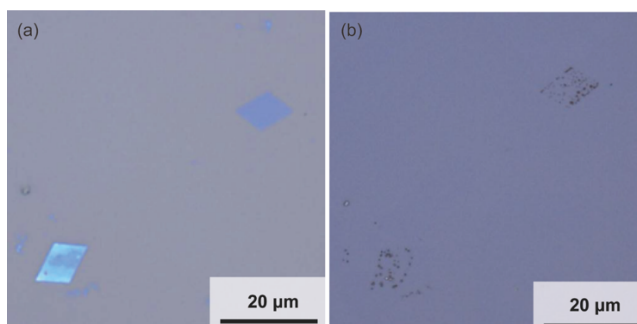


Fig.S 4 Appearances of the (a) 2D surfactant crystals and (b) those after reduction process without UV-ozone treatment.

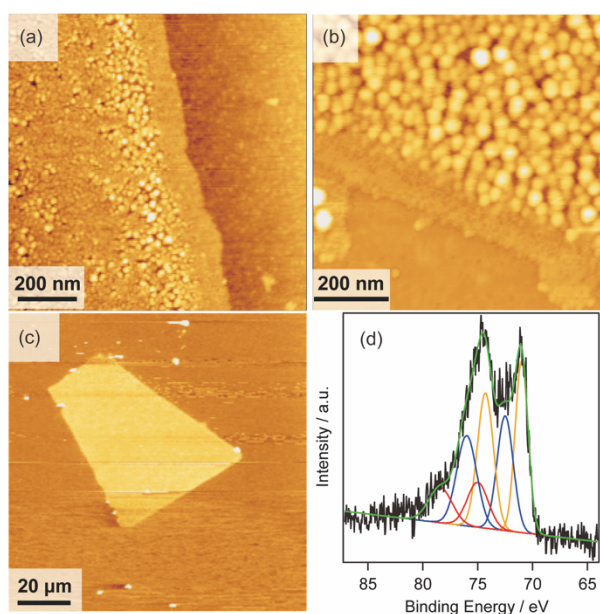


Fig.S 5 The AFM images of the Pt metal nanosheets reduced at (a) 200, (b) 300 and (c) 120 °C. (d) XPS spectrum of the Pt metal nanosheets reduced at 120 °C for 5 h.

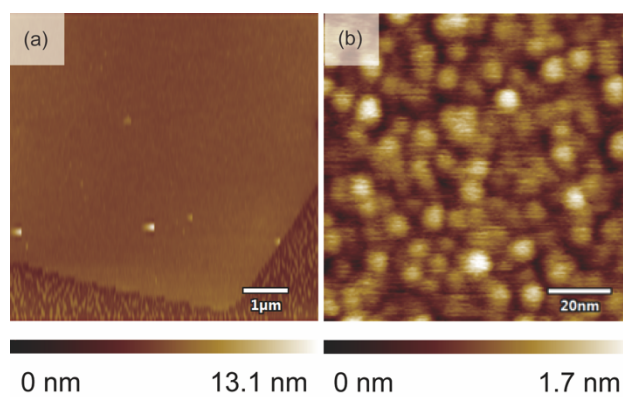


Fig.S 6 (a) AFM images and (b) its high-resolution image of Pt metal nanosheets synthesized on mica substrate. The images were observed by Cypher VRS equipment for clear observation of the nanostructure.

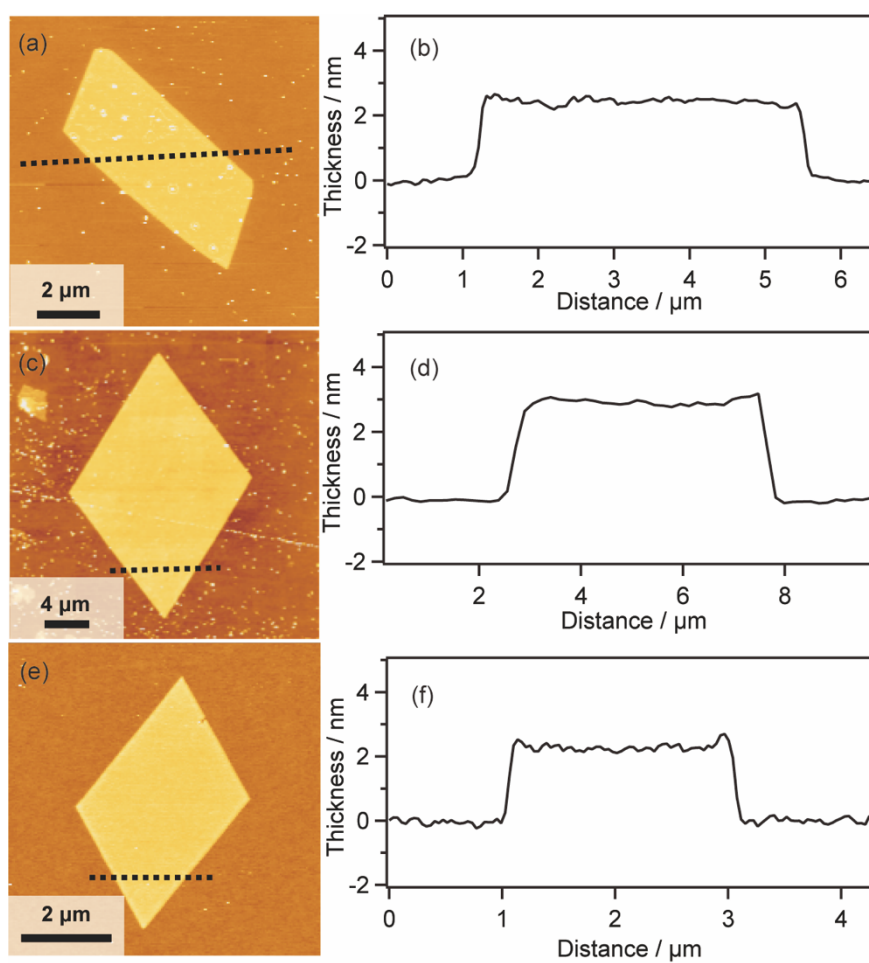


Fig.S 7 (a), (c), (e) and (g) AFM images and (b), (d), (f) and (h) height profiles of Pt metal nanosheets synthesized with various conditions: (a) and (b) nanosheet prepared on MgO substrate. (c) and (d) nanosheet prepared on  $\text{Al}_2\text{O}_3$  substrate. (e) and (f) nanosheet prepared using cetyltrimethylammonium chloride as a metal complex precursor.

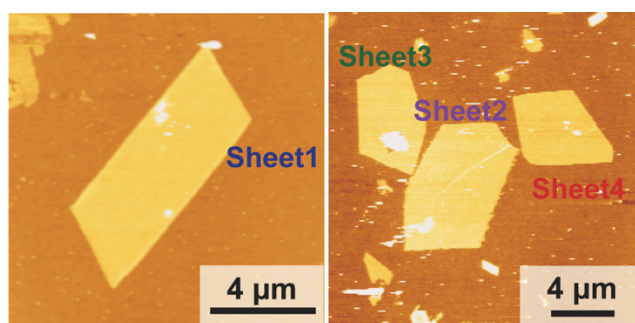


Fig.S 8 The AFM images of the Pt metal nanosheets used for monitoring the thicknesses.

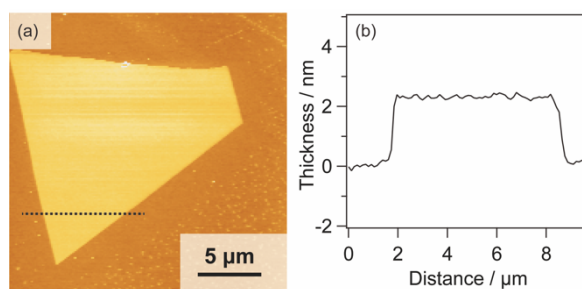


Fig.S 9 (a)AFM image and (b) height profile of the Pt metal nanosheet with large lateral size.

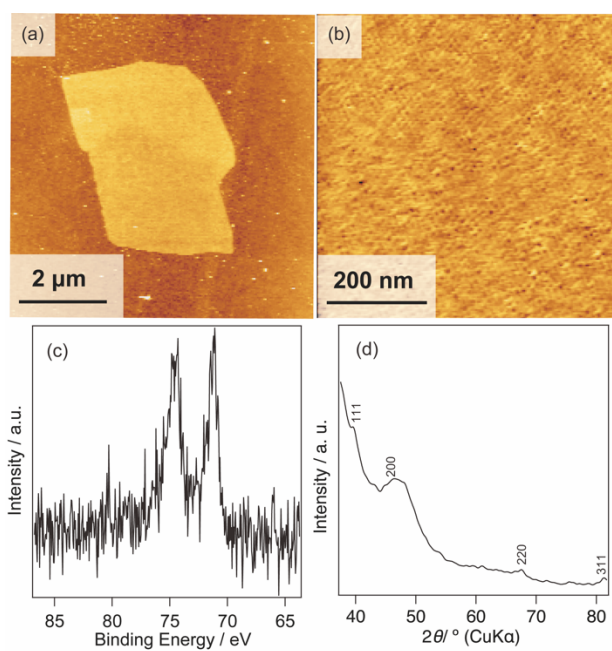


Fig.S 10 (a) and (b) AFM images, (c)XPS spectrum and (d) in-plane XRD pattern of Pt metal nanosheet after calcination.

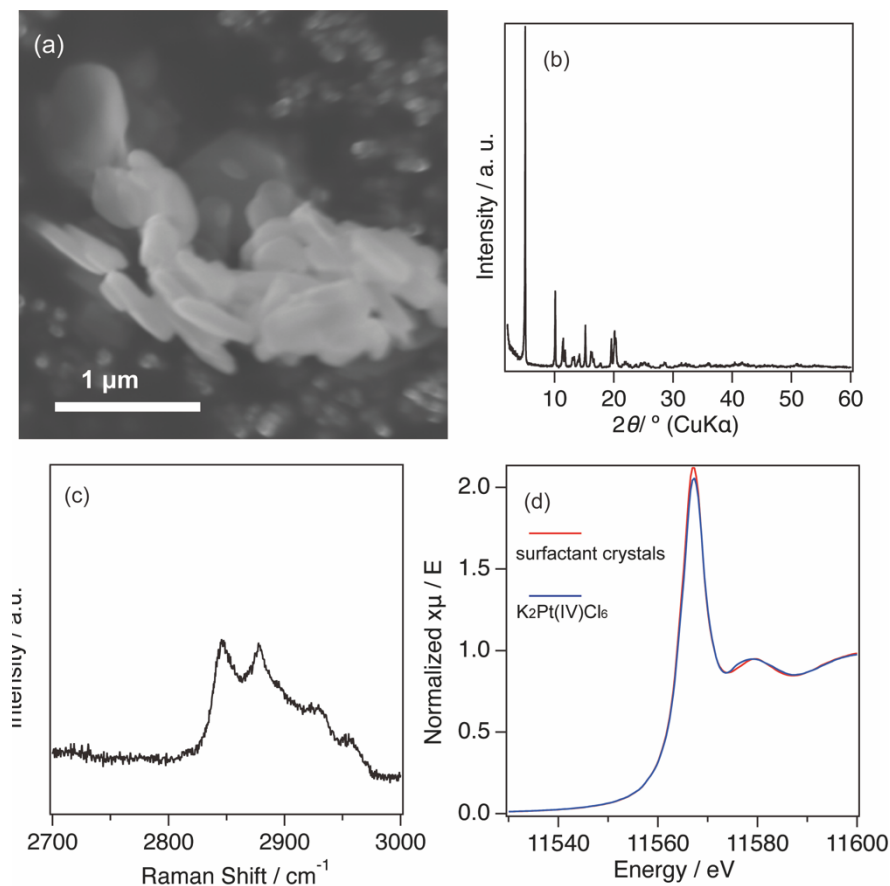


Fig.S 11 (a) SEM image (b) XRD pattern, (c) Raman spectrum, and (d) XANES spectrum of the surfactant crystals prepared using  $\text{H}_2\text{Pt(IV)Cl}_6$ .

#### Preparation of surfactant crystals using $\text{H}_2\text{Pt(IV)Cl}_6$

The formation of the surfactant crystals was confirmed by XANES and XRD measurements, Raman spectroscopy analysis and SEM observation. The surfactant crystals were prepared by mixing the aqueous solution of cetyltrimethylammonium bromide (CTAB) and  $\text{H}_2\text{Pt(IV)Cl}_6$ . The SEM image of the obtained powders showed the formation of platelet with 1  $\mu\text{m}$  in lateral size (Fig. S11 (a)). The XRD pattern of the obtained crystals showed clear peaks derived from the lamellar structure (Fig. S11 (b)). In addition, the peaks derived from the crystalline alkyl chain were also observed around  $22^\circ$ . These indicate the formation of the crystalline lamellar structure with Pt complex. The Raman spectrum showed clear peaks derived from the vibration of C-H groups, indicating the introduction of the surfactant (Fig. S10 (c)). In addition, the introduction of the Pt (IV) species was confirmed by XANES spectrum as confirmed because the spectrum almost traced the reference  $\text{H}_2\text{Pt(IV)Cl}_6$  (Fig. S10 (d)).



### Crystal Structure Refinement

CHN elemental analysis were conducted by a micro corder (J-science group JM10). Found: C, 49.23; H, 9.14; N, 3.11%.  $C_{38}H_{84}Br_{0.6}Cl_{3.4}N_2Pt$  requires C, 48.94; H, 9.08; N, 3.00 %. Elemental analysis using ion chromatography (Yanaco YHS-11) indicated the ratio of Br to Cl was 0.58:3.42. When the occupancies of the disordered Br and Cl sites ( $X1$  and  $X2$ ) were refined freely, the ratio of Br to Cl was 0.51:3.49. Reliable factors,  $R[F^2 > 2\sigma(F^2)]$ ,  $wR(F^2)$  and  $S$ , were 0.0198, 0.0455 and 1.062, respectively. All values are almost the same and the differences of the refined structures are within standard uncertainties. For the final step of the refinements, the ratio obtained by ion-chromatography were employed for refinement. Site occupancies of Br were refined as 0.2371(11) for  $X1$ , and 0.0627(11) for  $X2$ . Thus, Br prefers to occupy the  $X1$  site. When Br did not occupy at  $X2$  on the refinement,  $R[F^2 > 2\sigma(F^2)]$ ,  $wR(F^2)$  and  $S$  were 0.0224, 0.0567 and 1.055, respectively. The differences of the factors among the refined structures indicates that Br may exist at the  $X2$  site, even though the fraction is small. All nonhydrogen atoms were refined anisotropically and hydrogen atoms put using a riding model with appropriate instructions.

Table S1 Details of data collection and structure refinements

Crystal Data		
Chemical formula	$C_{38}H_{84}Br_{0.6}Cl_{3.4}N_2Pt$	
$M_r$	932.63	
Crystal system, space group	Triclinic, $P-1$	
Temperature / K	151	
$a, b, c$ / Å	7.59250(10), 20.0035(2)	8.14060(10),
$\alpha, \beta, \gamma$ / °	88.8910(10), 66.2290(10)	80.8020(10),
$V$ / Å <sup>3</sup>	1115.54(2)	
$Z$	1	
$D$ / g cm <sup>-3</sup>	1.388	
Radiation type	Mo $K\alpha$	
$\mu$ / mm <sup>-1</sup>	3.911	
Crystal size / mm	0.10 × 0.07 × 0.02	
$T_{min}, T_{max}$	0.723, 1.000	
No. of measured, independent	58022, 8515, 8475	

and observed [ $I > 2\sigma(I)$ ]

reflections

$R_{\text{int}}$  0.0342

$(\sin \theta/\lambda)_{\text{max}} / \text{\AA}^{-1}$  0.769

#### Refinement

$R[F^2 > 2\sigma(F^2)], wR(F^2), S$  0.0200, 0.0473, 1.035

No. of reflections 8515

No. of parameters 210

No. of restraints 1

H-atom treatment H-atom parameters constrained

$\Delta\rho_{\text{max}}, \Delta\rho_{\text{min}} / \text{e \AA}^{-3}$  2.06, -1.04

---

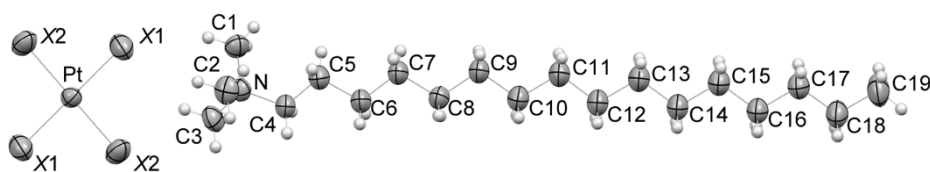


Fig.S 12 A moiety of  $[(\text{C}_{16}\text{H}_{33})\text{N}(\text{CH}_3)_3]_2[\text{PtX}_4]$  ( $\text{X} = \text{Br}$  or  $\text{Cl}$ ). Displacement ellipsoids are drawn at the 90% probability level.